Chapter 3
Estimation of the Dynamic Focused Ultrasound Radiation Force Generated by an Ultrasonic Transducer

Songmao Chen, Alessandro Sabato, and Christopher Niezrecki

Abstract Conventional excitation techniques such as modal impact hammer and shakers are commonly used in experimental modal testing. However, these excitation approaches require the excitation device to be in direct contact with test articles. It can result in distorted measurements, particularly for small structures, such as a MEMS cantilever and thumb nail size turbine blade. In addition, it is physically difficult or even impossible to apply these contact type excitations to some structures such as low stiffness structures or biological tissues. Moreover, these conventional excitations have limited bandwidth, usually less than 10 kHz, and thus are not applicable to extract information in higher frequency modes. Dynamic focused ultrasound radiation force has been recently used to excite structures with sizes ranging from micro to macro-scale and having a frequency bandwidth from tens of Hertz to up to 100 kHz. Therefore, it can potentially be used as an alternative, non-contact excitation method to these conventional contact excitation techniques for experimental modal analysis. Yet, this force remains to be quantified and calibrated in order to obtain the input-output relationship necessary to compute accurate frequency response functions of test structures. In this work a spherically focused ultrasound transducer (UT) is driven by double sideband suppressed carrier amplitude modulation (DSB-SC AM) signals with a scanning difference frequency and randomly varying carrier frequency. The radiated pressure field generated by the UT is experimentally measured employing a pressure microphone, which acts as a target object for the ultrasonic waves. Then, the recorded values are used to analytically evaluate the dynamic focused ultrasound radiation force. Results show that the measured radiation pressure and estimated force are characterized by a focal spot small enough to be compared to an impact hammer tip appropriate for future modal testing.

Keywords Radiation Force • Ultrasonic Transducer • Pressure Mapping • Force Estimation • Modal Analysis

3.1 Introduction

In recent years, a laboratory noncontact excitation method based on the focused ultrasound radiation force, generated by ultrasonic transducers (UT), has been explored to excite vibrations within structures with size ranging from micro scale (e.g. MEMS devices) to macro scale (e.g. guitars or engine turbine blades). The excitation frequency ranges from kHz to the MHz range and can potentially be used for modal testing. However, the lack of effective methods to quantify and calibrate the ultrasound radiation force prevents this approach from being used as a practical technique for measuring the frequency response functions (FRFs). Especially in modal testing analyses where the force input and response need to be measured in a synchronized manner.

In this paper, a review of previous research about the acoustic radiation force is presented in the first section. The mathematical description of the problem follows in the second section. The analytical quantification of the ultrasound radiation force in the focal plane generated by a spherically focused UT is addressed. After that, the experimental evaluation of the radiation pressure field generated by the UT is described. This is done by using calibrated radiation pressure fields resulting from the interaction between the incident ultrasound waves and the test articles. In particular, an acoustic microphone is used in these experiments for this purpose. The values of the measured radiation pressure field are then used to estimate the generated radiation force via the model described in Sect. 3.2. To finish, conclusions are drawn and a short description of future work is given in the final section.

S. Chen (✉) • A. Sabato • C. Niezrecki
Structural Dynamics and Acoustic Systems Laboratory, University of Massachusetts Lowell,
One University Avenue, Lowell, MA 01854, USA
e-mail: Songmao_Chen@student.uml.edu

E. Wee Sit et al. (eds.), *Sensors and Instrumentation, Volume 5*, Conference Proceedings of the Society for Experimental Mechanics Series, DOI 10.1007/978-3-319-54987-3_3

3.2 Prior Work

The acoustic radiation force [1–4] is generally interpreted as a time averaged force exerted by an acoustic field on targets standing in its propagating path. This force is an example of a universal phenomenon in any wave motion that causes some type of forces on absorbing or reflecting objects in the wave path [5, 6]. It can be understood from two different perspectives: the energy standpoint and the viewpoint of dynamics. According to the former, this force is generated by a change in the energy density of incident waves; while for the latter, when acoustic waves hit an object, part of the momentum carried by the waves is transferred to the object. Lord Rayleigh was the first to propose a theory for acoustic radiation force in lossless fluids due to compressional waves [1, 2]. For over a century since that seminal work, the acoustic radiation forces on planar objects, spheres, cylinders, and shells have been undergone extensive investigation by a large number of researchers, mostly in theoretical aspect [7, 8]. In most cases, incident travelling plane waves were assumed while nonplanar waves such as focused beams were considered in very limited cases [9–11]. A detailed theoretical analysis of acoustic radiation force acting on a rigid sphere by plane waves was first presented by King [12]. This was then extended to include the effect of the compressibility of spheres by Yosioka and Kawasima [13]. Following that, Hasegawa and Yosioka [14, 15] conducted theoretical and experimental research on the radiation force experienced by an isotropic elastic sphere. Later on, they studied the acoustic radiation force acting on a rigid cylinder by travelling planes waves [16] and subsequently extended it to take into account the cylinder's elasticity [17]. The effects of dissipative factors such as viscosity and heat transfer were also studied and it was found that they could drastically affect the resulting acoustic radiation force [10, 18, 19].

To the authors' knowledge, the previous studies assumed evenly and symmetrically distributed pressure fields, and yet in practice, this assumption is not always valid for real operating UTs. There are a variety of methods to map sound fields generate from UTs, such as interferometer [20], light synchronization [21], acoustic array [22], and acoustically induced piezo-luminescence [23], etc. Chen et al. studied the vibrations and acoustical characteristics of an airborne plane circular transducer using numerical modelling and experimental mapping techniques. It was found that the transducer's emitting surface was not in uniform and symmetrical vibration and the generated acoustic spot was not exactly in the geometrical center [24, 25]. A preliminary study on the structural dynamics and acoustical performance of a spherically focused ultrasonic transducer by the authors also shows that the focal spot is actually shifted from the geometrical center in the focal plane [26]. Huber et al. used the measured vibrational response to estimate the force imparted to a rectangular plate in an inverse manner [27].

3.3 Theoretical Background

For an ideal fluid, in which the thermal and viscous effects are neglected, its dynamics are described by the principle of mass conservation, momentum conservation (Newton's Second Law in fluid dynamics), and Poisson's equation in Eqs. (3.1), (3.2), and (3.3), respectively.

$$\frac{\partial \rho}{\partial t} + \nabla \cdot (\rho \boldsymbol{v}) = 0 \tag{3.1}$$

$$\rho \frac{d\boldsymbol{v}}{dt} = -\nabla p \tag{3.2}$$

$$p = p_0 \left(\frac{\rho}{\rho_0} \right)^{\gamma} \tag{3.3}$$

where p_0 and ρ_0 are the fluid pressure and density in initial equilibrium state, respectively, $\boldsymbol{v}$ is particle velocity, and γ the ratio of specific heat.

The particle velocity in an ideal fluid, according to the Helmholtz vector theorem, can described as a function of the velocity potential Φ,

$$\boldsymbol{v} = -\nabla \Phi = -\nabla \left(\Phi_1 + \Phi_2 + \cdots \right) \tag{3.4}$$

where Φ_1 and Φ_2 are the first order (linear) and second order velocity potentials, respectively.

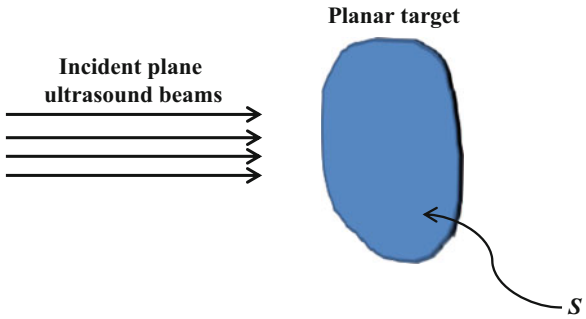

Fig. 3.1 Schematic of incident plane ultrasound beams impinging on a planar target

The pressure variation, or excess pressure δp, is given to the second order of $\boldsymbol{v}$ by

$$\delta p = p - p_0 = \rho_0 \left(\dot{\Phi}_1 + \dot{\Phi}_2\right) - \frac{1}{2}\rho_0 \boldsymbol{v}_1^2 + \frac{1}{2}\frac{\rho_0}{c_0}\dot{\Phi}_1^2 \tag{3.5}$$

where $\boldsymbol{v}_1 = \nabla\, \Phi_1$ is the first order particle velocity, and $\dot{\Phi}_i$ is the first partial derivative of the velocity potential.

Radiation force is a nonlinear phenomenon that relies on the interaction between the second order acoustic field and target objects. Assuming that a closed boundary S in the medium is in motion with a small velocity of $\boldsymbol{v}_1$. The acoustic radiation force on the moving boundary to the second order is expressed by

$$\boldsymbol{F} = -\iint_S \delta p \mathbf{n} ds = \left(-\iint_S \rho_0 \dot{\Phi}_1 \mathbf{n} ds\right) + \left(-\iint_{S_0} \rho_0 \dot{\Phi}_2 \mathbf{n} ds\right) + \iint_{S_0} \frac{1}{2}\rho_0 v_1^2 \mathbf{n} ds + \left(-\iint_{S_0} \frac{1}{2}\frac{\rho_0}{c_0}\dot{\Phi}_1^2 \mathbf{n} ds\right) \tag{3.6}$$

where S_0 represents the initial boundary in equilibrium status [13].

The acoustic radiation force is usually a steady (or static) force [2–6], generated by a monochromatic continuous wave sound beam, the intensity of which does not vary over time [28]. Consider plane ultrasound beams impinging on a planar target of zero thickness, arbitrary shape and boundary impedance that scatters and absorbs, as shown in Fig. 3.1.

The acoustic radiation force vector, $\boldsymbol{F}$, arising from these interactions has two components: one in the beam's incident direction and another transverse to it. The magnitude of this force, derived from the Eq. (3.6), is proportional to the time-averaged energy density of the incident wave $\langle E \rangle$ at the object and the area of the projected portion of the object S, as shown in the Eq. (3.7) below [3, 29–31]

$$\boldsymbol{F} = \langle E \rangle\, S \boldsymbol{d}_r \tag{3.7}$$

where $\langle\rangle$ indicates the time average, and $\boldsymbol{d}_r$ is the vector drag coefficient with a component in the direction of the incident wave and another transverse to the incident beam. The coefficient $\boldsymbol{d}_r$ is defined per unit incident energy density and unit projected area, and its magnitude is dependent upon a variety of factors such as the shape of target objects and the direction of propagating waves [26]. In particular, for a planar object of perfect absorption, $\boldsymbol{d}_r = 1.0$, while for a planar object of perfect reflection, $\boldsymbol{d}_r = 2.0$. When it is assumed that a planar object is oriented that its outward normal direction is parallel and inverse to the incident beam axis, the transverse component of radiation force disappears. In this case, the drag coefficient, as well as the force, retains the component normal to the target surface only.

The goal of this research is to use a UT for producing waves to excite structures. To do so, the generation of a dynamic ultrasound radiation force is necessary. This can be achieved using three different beam forming methods: amplitude-modulated (AM) beams, confocal beams, and x-focal beams [32]. In this work, a single focused ultrasonic transducer is used and a double sideband suppressed-carrier (DSB-SC) AM signal is used as the excitation [32]. In particular, an excitation signal having two component frequencies: f_1 and $f_2 = f_1 + \Delta f$, has been used to generate a pair of UT waves characterized by these frequency components. When a structure is ensonified by this pair of ultrasound beams, interference between the beams and interactions between the beams and the structure yield to a radiation force that vibrates the structure at the difference frequency $\Delta f = f_2 - f_1$. Assuming that the sound pressure P($\mathbf{r}$) at the observation point $\mathbf{r}$ in the ultrasound field are the same at both frequencies that are emitted by the transducer, the total pressure field due to the two frequency components may be written as

$$p(\boldsymbol{r},t) = P(\boldsymbol{r})\cos\left[2\pi f_1 t + \varphi_1(\boldsymbol{r})\right] + P(\boldsymbol{r})\cos\left[2\pi f_2 t + \varphi_2(\boldsymbol{r})\right] \tag{3.8}$$

This equation, also considers that when two waves of different frequencies travel the distance between the transducer and the destination point **r**, they will have different phases $\varphi_1(\mathbf{r})$ and $\varphi_2(\mathbf{r})$.

This produces an instantaneous energy density represented by

$$E(\boldsymbol{r},t) = p^2(\boldsymbol{r},t)/\rho c^2 \tag{3.9}$$

where ρ and c are the density of and speed of sound in the fluid. This energy density will have a time independent (static) component, a component at the difference frequency Δf, and higher frequency components at $f_1 + f_2$ and multiples of f_1 and f_2.

In this work, Δf is the frequency of interest of the structure, and since it is significantly lower than f_1 and f_2, the part of radiation force corresponding to higher frequency energy components will hardly contribute to the vibration of the test structure. The radiation force associated with the energy density component at the difference frequency is represented by

$$E_{\Delta f}(\boldsymbol{r},t) = P^2(\boldsymbol{r})\cos\left[2\pi\Delta f t + \Delta\varphi(\boldsymbol{r})\right]/\rho c^2 \tag{3.10}$$

where $\Delta\varphi(\mathbf{r})$ is the difference phase at the observation point, $\Delta\varphi(\mathbf{r}) = \varphi_1(\mathbf{r}) - \varphi_2(\mathbf{r})$.

Assuming that P($\boldsymbol{r}$) is a plane wave, according to the Eq. (3.7) a force in the propagating direction of the incident beams will be imparted on the structure of area ds with drag coefficient $d_r(\boldsymbol{r})$

$$F_{\Delta f}(\boldsymbol{r},t) = E_{\Delta f}(\boldsymbol{r},t)\,dS\;\; d_r(\boldsymbol{r}) = P^2(\boldsymbol{r})\cos\left[2\pi\Delta f t + \Delta\varphi(\boldsymbol{r})\right]/\rho c^2\;\; d_r(\boldsymbol{r})\,dS \tag{3.11}$$

The overall radiation force as a function of time can be obtained by integrating Eq. (3.11) over the impacted surface of the test structure, which will be vibrated at the difference frequency Δf. The structural vibration caused by this radiation force is a function of the size, shape, and mechanical impedance of the test structure.

Another term, referred to as the average radiation pressure P^R, is governed by the following equation

$$P^R_{\Delta f}(\boldsymbol{r}) = P^2(\boldsymbol{r})\cos\left[2\pi\Delta f t + \Delta\varphi(\boldsymbol{r})\right]/\rho c^2\;\; d_r(\boldsymbol{r}) \tag{3.12}$$

In this work, the average radiation pressure is what the measuring microphones capture. By integrating the radiation pressure over the impacting surface, the radiation force is estimated, as indicated in Eq. (3.13).

$$F_{\Delta f}(\boldsymbol{r},t) = \iint_S P^R_{\Delta f}(\boldsymbol{r})\,ds \tag{3.13}$$

This final equation will be used for computing the force distribution in the focal plane of the UT.

3.4 Experiments and Setup

Most of the work previously done has focused on the theoretical analysis of the acoustic radiation pressure and/or force. Instead, this study aims to find a way to indirectly evaluate the acoustic force acting on the test structure starting from the analysis of the pressure field generated by the focused UT. For this reason, an acoustic microphone has been used to map the radiation pressure resulting from the interaction between the ultrasound waves and the microphone, which acts as the test structure. The schematic diagram and the experimental setup used for performing this test are shown in Fig. 3.2. The excitation signal, produced by a signal generation card manufactured by The Spectrum Instruments Inc., is a double sideband suppressed-carrier (DSB-SC) with amplitude modulation (AM). This beam forming method has been selected because it can generate a signal having two frequencies using only one focal UT. For the DSB-SC excitation signal, the carrier frequency is centered at 359 kHz with a random variation of 20 kHz. It should be pointed out that a random variation in the carrier frequency helps to prevent interference between the incident and reflected waves that can lead to standing waves. As a result, the difference frequency Δf acting on the microphone can vary from 100 Hz to more than 20 kHz. The signal is then fed into a focused UT after being amplified by a power amplifier (240 L, E&I Ltd). The UT used was a NCG500-D50-P150 model from the Ultran Group with a focal length of approximately 150 mm. A B&K acoustic microphone (Type 4939) has been

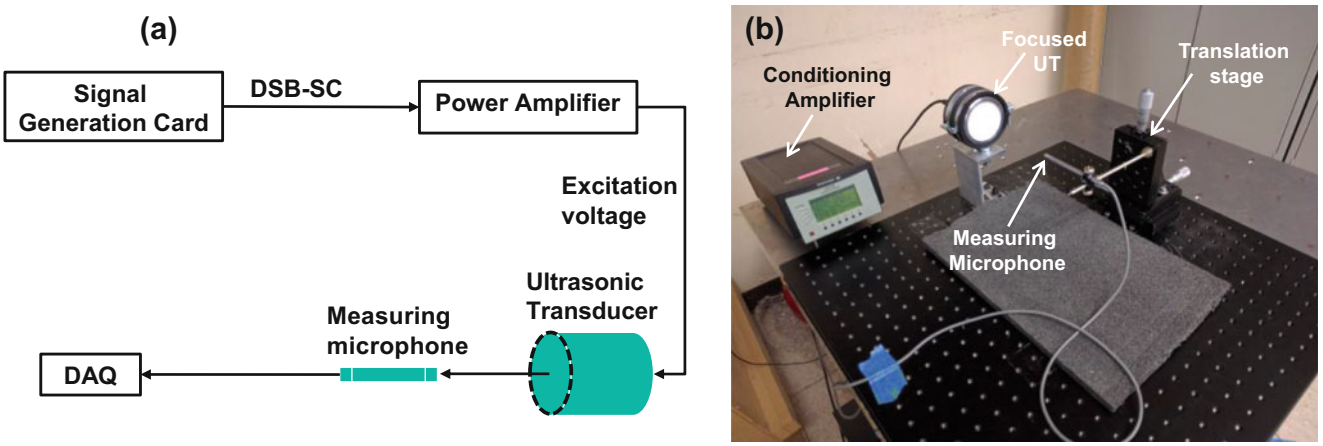

Fig. 3.2 The radiation pressure mapping using acoustic microphone. (**a**) Schematic diagram; (**b**) experimental setup

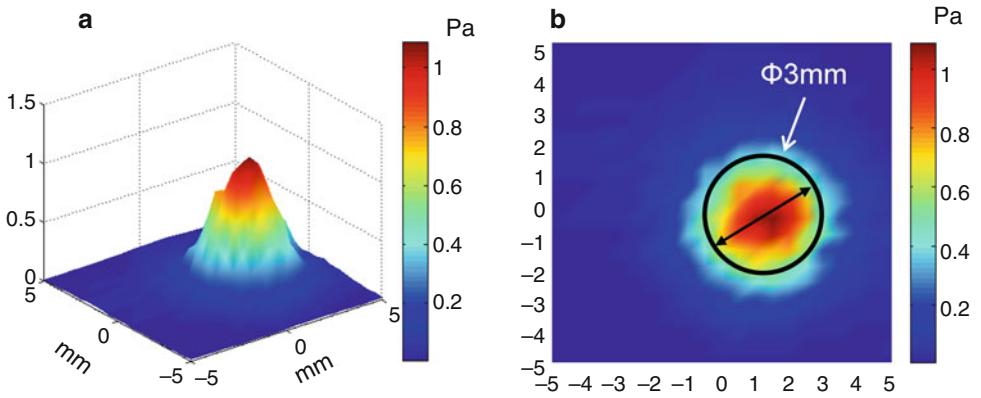

Fig. 3.3 The radiation pressure field at the difference frequency of 372 Hz in the focal plane. (**a**) Isometric view; (**b**): Top view

used to map the produced radiation pressure profile and the results are acquired by the PSV acquisition software (Polytec Inc.). In the experiment, the measuring microphone is acting like a test target placed in the focal plane of the transducer, ∼150 mm away from the center of the transducer itself. The size of the measurement plane selected for the test is 5 × 5 mm with the spatial resolution of 0.5 mm.

A specific example of the performed measurements is provided below. It refers to the radiation pressure field measured by the acoustic microphone at $\Delta f = 372$ Hz (i.e. the resonance frequency of the first mode of a test structure to be investigated in future test planned to validate this technique) in the focal plane and it is shown in Fig. 3.3.

The results indicate that the radiation pressure field has spot size of ∼3 mm in diameter (the size of the focal spot is delimited by the area in which the ratio of pressure to the peak value is higher than 0.2). In particular, it can be observed that the acoustic spot has a peak value of ∼1.2 Pa and it is located at (1.5, 0) mm viewing from the top, rather than in the geometrical center. This finding further validates the author's assumption that real operating UTs do not always generate evenly and symmetrically distributed pressure fields, and research in this field are useful for a better understanding about the acoustic performance of UTs.

3.5 Force Estimation and Discussion

By using Eq. (3.13), i.e., integrating the measured ultrasound radiation pressure over corresponding surface area, we are able to compute the spatial distribution of the ultrasound radiation force, or the force intensity distribution. Results are plotted in Fig. 3.4. It can be seen that the majority of the radiation force is focused on the acoustic spot, the very center of which (i.e. around the point at (1.5, 0) ±0.5 mm) has an intensity of 2.6E-5 N.

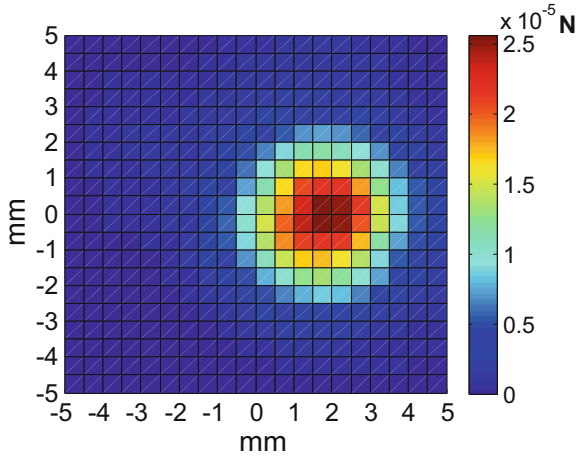

Fig. 3.4 The spatial distribution of the ultrasound radiation force corresponding to the radiation pressure field in Fig. 3.3

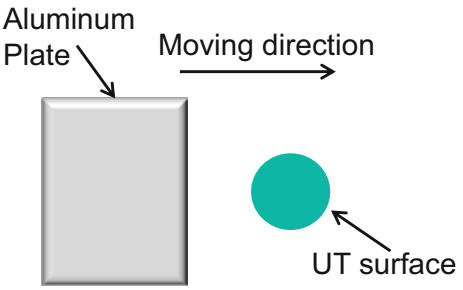

Fig. 3.5 Schematic of roving an aluminum plate across the UT

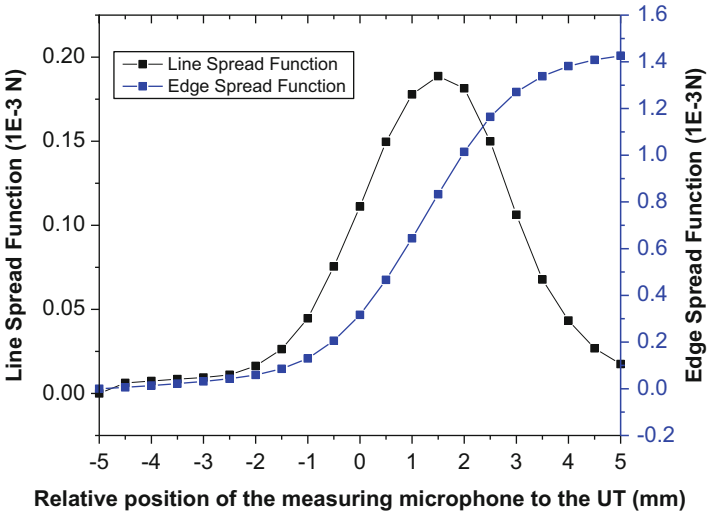

Fig. 3.6 The ultrasound radiation force: edge spread function and line spread function obtained for a difference frequency of 372 Hz

One way to examine the radiation force characteristics of an UT is to observe the edge spread function (ESF) and line spread function (LSF) [27]. Let us imagine roving a rectangular plate across the UT surface from left to right as shown in Fig. 3.5.

The radiation force produced by the UT and acting on the plate can be calculated using a 2D integral of the radiation pressure similar to that shown in Eq. (3.13). The accumulated radiation force, computed from the left edge to the position where the plate is currently located, is referred to as the edge spread function (ESF). The values of the ESF for different position of the plate are plotted using the blue curve in Fig. 3.6.

It is possible to observe that the radiation force has a maximum of $\sim$1.4E-3 N when the plate covers the whole surface of the UT (i.e. the plate's edge is in correspondence of $+5$ mm). This technique allows detecting when the test object is completely within the pressure filed generated by the transducer, and allows maximizing the effects of the excitation. When

a slice of the plate having a width of 0.5 mm is considered, it is possible to evaluate the LSF. It is a measure of the radiation force acting on each slice caused by the radiation pressure field, and it can be calculated as the derivative of the ESF with respect to the position. As can be seen in Fig. 3.6, the LSF maximum value is centered on x = 1.5 mm and its intensity is equal to 0.18E-3 N, confirming the position of the focal spot computed using the microphone. This technique shows that is possible to highlight the real focal spot position of an UT, by simply swiping a piece of metal in front of the transducer and looking for the maximum response.

3.6 Conclusions

In this work, the theory of the ultrasound radiation force is discussed and a method for analytically estimating its intensity from experimental results is presented. This technique allows characterizing the force an ultrasound transducer applies on a test structure which can be used as novel excitation technique for modal analysis. Experiments are performed to measure the generated radiation pressure field when the UT is driven with double sideband suppressed-carrier (DSB-SC) with amplitude modulation signal having a carrier frequency of 359 kHz. Based on the measured radiation pressure profile, the radiation force is quantified using an analytical method. Results show that the resulting radiation pressure and force have a focal spot with a size of $\sim$3 mm in diameter. This spot is highly focused and its dimensions are comparable to those of impact hammer tips and impedance head of shakers. Therefore, if further investigate, this this force estimation method may lead to the calculation of the force input-output response relationship (i.e. frequency response functions) in experimental modal analysis and identify structural dynamics parameters in a non-contact manner.

Acknowledgements The authors are grateful for the financial support by the NSF under Grant No. CMMI-1266019. We also appreciate the many discussions with Prof. Peter Avitabile, Patrick Logan, Tina Dardeno, and Peyman Poozesh. Any opinions, findings, and conclusions or recommendations expressed in this material are those of the authors and do not necessarily reflect the views of the National Science Foundation.

References

1. Rayleigh, L.: XXXIV. On the pressure of vibrations. London Edinburgh Dublin Philos. Mag. J. Sci. **3**(15), 338–346 (1902)
2. Rayleigh, L.: XLII. On the momentum and pressure of gaseous vibrations, and on the connexion with the virial theorem. London Edinburgh Dublin Philos. Mag. J. Sci. **10**(57), 364–374 (1905)
3. Westervelt, P.J.: The theory of steady forces caused by sound waves. J. Acoust. Soc. Am. **23**(3), 312–315 (1951)
4. Westervelt, P.J.: Acoustic radiation pressure. J. Acoust. Soc. Am. **29**(1), 26–29 (1957)
5. Torr, G.: The acoustic radiation force. Am. J. Phys. **52**(5), 402–408 (1984)
6. Chu, B.T., Apfel, R.E.: Acoustic radiation pressure produced by a beam of sound. J. Acoust. Soc. Am. **72**(6), 1673–1687 (1982)
7. Beyer, R.T.: Radiation pressure—the history of a mislabeled tensor. J. Acoust. Soc. Am. **63**(4), 1025–1030 (1978)
8. Mitri, F.: Axial time-averaged acoustic radiation force on a cylinder in a nonviscous fluid revisited. Ultrasonics. **50**(6), 620–627 (2010)
9. Wu, J., Du, G.: Acoustic radiation force on a small compressible sphere in a focused beam. J. Acoust. Soc. Am. **87**(3), 997–1003 (1990)
10. Rudenko, O., Sarvazyan, A., Emelianov, S.Y.: Acoustic radiation force and streaming induced by focused nonlinear ultrasound in a dissipative medium. J. Acoust. Soc. Am. **99**(5), 2791–2798 (1996)
11. Beissner, K.: Radiation force calculations for ultrasonic fields from rectangular weakly focusing transducers. J. Acoust. Soc. Am. **124**(4), 1941–1949 (2008)
12. King, L.V.: On the acoustic radiation field of the piezo-electric oscillator and the effect of viscosity on transmission. Can. J. Res. **11**(2), 135–155 (1934)
13. Yosioka, K., Kawasima, Y.: Acoustic radiation pressure on a compressible sphere. Acta Acust. United Acust. **5**(3), 167–173 (1955)
14. Hasegawa, T., Yosioka, K.: Acoustic-radiation force on a solid elastic sphere. J. Acoust. Soc. Am. **46**(5B), 1139–1143 (1969)
15. Hasegawa, T.: Comparison of two solutions for acoustic radiation pressure on a sphere. J. Acoust. Soc. Am. **61**(6), 1445–1448 (1977)
16. Hasegawa, T., Saka, K., Inoue, N., et al.: Acoustic radiation force experienced by a solid cylinder in a plane progressive sound field. J. Acoust. Soc. Am. **83**(5), 1770–1775 (1988)
17. Hasegawa, T., Hino, Y., Annou, A., et al.: Acoustic radiation pressure acting on spherical and cylindrical shells. J. Acoust. Soc. Am. **93**(1), 154–161 (1993)
18. Doinikov, A.A.: Acoustic radiation pressure on a compressible sphere in a viscous fluid. J. Fluid Mech. **267**, 1–22 (1994)
19. Settnes, M., Bruus, H.: Forces acting on a small particle in an acoustical field in a viscous fluid. Phys. Rev. E. **85**(1), 016327 (2012)
20. Nemoto, M., Mizutani, K., Ezure, T., et al.: Measurement of sound fields using Mach–Zehnder interferometer. Jpn. J. Appl. Phys. **43**(9R), 6444 (2004)
21. Yao, G., Wang, L.V.: Full-field mapping of ultrasonic field by light-source-synchronized projection. J. Acoust. Soc. Am. **106**(4), L36–L40 (1999)
22. Aizawa, K., Poozesh, P., Niezrecki, C., et al.: An acoustic-array based structural health monitoring technique for wind turbine blades, in SPIE/NDE, San Diego, 2015

23. Kersemans, M., Smet, P.F., Lammens, N., et al.: Fast reconstruction of a bounded ultrasonic beam using acoustically induced piezoluminescence. Appl. Phys. Lett. **107**(23), 234102 (2015)
24. Chen, S., Niezrecki, C., Avitabile, P.: Experimental mapping of the acoustic field generated by ultrasonic transducers. In The 34th International Modal Analysis Conference, Orlando, 2016
25. Chen, S., Niezrecki, C., Avitabile, P., et al.: Numerical simulation and dual experimental mapping of acoustic field generated by ultrasonic transducers. Proc. Inter-Noise Noise-Con. **525**(2), 849–856 (2016)
26. Chen, S., Sabato, A., Niezrecki, C., et al.: Modelling and experimental mapping of the ultrasound pressure field generated from focused ultrasonic transducers using fiber optic acoustic sensors. In 172nd Meeting of the Acoustical Society of America, Honolulu, 2016
27. Huber, T. M., Algren, M., Raisbeck, C.: Spatial distribution of acoustic radiation force for non-contact modal excitation. In The 34th International Modal Analysis Conference, Orlando, 2016
28. Chen, S., Silva, G.T., Kinnick, R.R., et al.: Measurement of dynamic and static radiation force on a sphere. Phys. Rev. E. **71**(5), 056618 (2005)
29. Fatemi, M., Greenleaf, J.F.: Ultrasound-stimulated vibro-acoustic spectrography. Science. **280**(5360), 82–85 (1998)
30. Fatemi, M., Greenleaf, J.F.: Vibro-acoustography: an imaging modality based on ultrasound-stimulated acoustic emission. Proc. Natl. Acad. Sci. **96**(12), 6603–6608 (1999)
31. Fatemi, M., Greenleaf, J.F.: Probing the dynamics of tissue at low frequencies with the radiation force of ultrasound. Phys. Med. Biol. **45**(6), 1449 (2000)
32. Chen, S., Fatemi, M., Kinnick, R., et al.: Comparison of stress field forming methods for vibro-acoustography. IEEE Trans. Ultrason. Ferroelectr. Freq. Control. **51**(3), 313–321 (2004)